In order that ψ may have both a maximum and a minimum, the intercept, f, of the straight line (3) on the z-axis must lie between $f_0=0F_0$ and $f_1=0F_1$. The tangent TCF_1 and the line AF_0B in Fig. 2 mark the extreme positions of (3). From the condition of tangency of line (3) to curve (2), it may be shown that for the position TCF_1 of (3), the amplitude E^* of the electric field in Eq. (15), Sec. 4, vanishes.

When the line (3) lies between TCF_1 and AF_0B, the maxima and minima of $\psi(\xi)$ occur at different values of ψ. So long as (3) lies near TCF_1 (small E^*), the difference between ψ_{max} and ψ_{min} is small, and the oscillation may be considered simple harmonic. With increasing E^*, however, the maxima and minima get progressively further apart, and the oscillation becomes increasingly anharmonic.

The point F_0 is obtained from the intersection of (3) with (2) at $\psi=-b$. This gives

$$f_0=0F_0=b+c(d-b)^{\frac{1}{2}}. \tag{4}$$

When the line (3) intercepts the z-axis below $0F_0$, ψ has a maximum but does not reach the minimum given by the vanishing of (1), as $d\psi/d\xi$ in (1) becomes imaginary when $\psi<-b$. The oscillation curve of ψ has the form shown in Fig. 3. There is a discontinuity in $d\psi/d\xi$ and hence in the electric field at the minima of ψ (A in Fig. 3).

PHYSICAL REVIEW VOLUME 97, NUMBER 4 FEBRUARY 15, 1955

Transmission of Slow Neutrons by Liquid Helium*

HENRY S. SOMMERS, JR.,† J. GREGORY DASH, AND LOUIS GOLDSTEIN
University of California, Los Alamos Scientific Laboratory, Los Alamos, New Mexico
(Received May 24, 1954)

We have determined the total scattering cross section of liquid helium for neutrons of wavelengths between 3 and 16 angstroms and at six helium temperatures between 1.25 and 4.6°K. The neutrons were obtained from the thermal beam of a reactor and were monochromatized by a low resolution velocity selector. The total scattering cross section decreases with temperature at all wavelengths studied. At the shortest wavelengths the cross section approximates the free atom value; it exhibits a rapid drop with increasing wavelength. For the 4.6° liquid it passes through a shallow minimum at about 10 A. At lower helium temperatures, the fall from the free atom cross section is steeper; the existence of a minimum has not been established. The results are discussed qualitatively on the basis of several models of liquid helium. The only one predicting the overall features of the change of cross section with wavelength and temperature is the solid model.

1. INTRODUCTION

IN general, experimental investigations of the properties of liquid helium[1] use methods whereby gross or average properties are studied. Even in the investigations of the saturated and unsaturated helium film,[2] and in studies of first and second sound,[3] the thickness of the film or the wavelength of the periodic motions has been many atomic distances. Hence, these experiments involve sufficiently large numbers of atoms to permit a first treatment by thermodynamics.

An exception to this generalization is the studies of scattering of x-rays and slow neutrons by liquid helium. When the wavelength of the incident radiation is comparable with the atomic spacing, the observed phenomena are governed by the local or atomic rather than the bulk properties. Such studies help to reveal the atomic properties of the liquid, the spatial arrangement of the atoms, the mean forces between them, their mean velocity, and kinetic energy. They might even yield the laws of their velocity distribution.

Neutron scattering studies are of interest, not primarily as an independent check or improvement on x-ray results, but to complement them. Aside from electronic excitation, the vanishing rest mass of the photons inhibits the exchange of energy with the liquid. In addition, the velocities of photon and molecule are so different that the internal motion of the scatterer is unimportant. Because of these facts, the x-ray diffraction pattern is, essentially, the momentum space Fourier transform of the static radial distribution of the atoms around one chosen arbitrarily, as first shown by Zernike and Prins.[4] Many workers have used this transformation to derive the pair distribution from the scattering diagrams.[5] In the case of the scattering of slow neutrons, however, the masses and velocities of incident particle and scatterer may be comparable. As discussed later

* This paper has been reported on at the Washington, D. C. meeting of the American Physical Society, April 30–May 1, 1953 [Phys. Rev. 91, 490 (1953)].
† Present address: RCA Research Laboratories, Princeton, New Jersey.
[1] W. H. Keesom, *Helium* (Elsevier, Amsterdam, 1942).
[2] See the review of E. A. Long and L. Meyer, Phil. Mag. Supplement 2, 1 (1953).
[3] For a recent survey see K. R. Atkins, Phil. Mag. Supplement 1, 169 (1952).
[4] F. Zernike and J. A. Prins, Z. Physik. 41, 184 (1927).
[5] See the review of N. S. Gingrich, Revs. Modern Phys. 15, 90 (1943).

the neutron scattering cross section then depends on the forces between the atoms and the energy states of the liquid as well as on the spatial distribution of the atoms. A suitable analysis of x-ray and slow neutron scattering experiments may yield information about a number of fundamental molecular properties of liquids.[6,7]

The first studies of x-ray diffraction by liquid helium were made by Keesom and Taconis and by Reekie.[8] Neither investigation found any influence of the lambda transition on the diffraction patterns. The atomic pair distribution function in liquid helium has been derived by Reekie and his collaborators[9] from their new x-ray investigations. Again the lambda transition was undetectable.

The slow neutron scattering by liquid helium has only recently been studied. In a survey of the total scattering cross section of liquid helium using graphite filtered slow neutrons,[10] the cross section decreased rapidly with increasing neutron wavelength, making the helium sample transparent. In addition to this, no appreciable change in scattering occurred in the vicinity of the lambda point.

Henshaw and Hurst[11] have given a preliminary report of the angular scattering of slow neutrons by liquid helium at 1.2°K, using 1.08 A neutrons. When completed, their work should yield the pair distribution function, but as yet insufficient data is available. London and Egelstaff,[12] using beryllium filtered neutrons of about 4.6 A mean wavelength, have studied the small angle forward and backward scattering at a number of temperatures from 1.6 to 5.2°K. They found that the liquid acts like a collection of free atoms (backward scattering), or of bound atoms (forward scattering) with which chiefly momentum is exchanged. This was to be expected on theoretical grounds.[6] In neither of these experiments can much information be derived about the forces or energies of the liquid atoms.

The present work is a refinement of our preliminary measurements[10] of the total scattering cross section. By a great increase of the path length in liquid helium and the use of a neutron velocity selector, we have obtained quantitative answers about the effects of the lambda transition and the helium temperature on the scattering and about the interaction of the helium atoms with neutrons of comparable velocities. Part I of this paper presents these measurements as well as a qualitative comparison between the results and the predictions of several models of liquid helium. Part II[13] will be devoted to an analysis of the cross sections according to a more general theoretical approach, valid, within limitations, in all monatomic liquids. There, the mean kinetic energy, zero point energy included, and the mean square force on a liquid atom are derived.

2. EXPERIMENTAL ARRANGEMENT

A. Apparatus

The experimental arrangement is shown schematically in Fig. 1. The neutrons emanating from the active sphere at the center of the Supo reactor[14] are moderated to an approximately Maxwellian velocity distribution by seven inches of heavy water. The thermalized beam is collimated by a $1\frac{5}{8}$-inch diameter hole through the thermal column. In order to minimize absorption in atmospheric nitrogen, a thin walled aluminum tube filled with helium gas was inserted in this hole. The emerging beam passes successively through a velocity selector, additional collimators, the liquid helium target, and a neutron counter.

The external beam collimation is achieved by a $1\frac{3}{8}$-inch diameter hole in a lucite block seven inches long, faced with $\frac{1}{32}$-inch cadmium sheets with $1\frac{1}{4}$-inch holes. A pair of these blocks encloses the cryostat. The overall collimator geometry yields an effective beam divergence of half-angle about 0.004 radians as seen by the counter.

The neutron detector is a brass end-view counter $1\frac{1}{2}$ inches in diameter by 1 inch active length, filled to a pressure of 35 cm Hg with BF_3 gas enriched to 95 percent B^{10}. The very short active length slightly decreased the counting rates but gave a large reduction in background of epi-cadmium neutrons. Further reduction in the background was achieved by embedding the counter in a cubic foot of paraffin lined inside and out with cadmium. Tests showed that most of the remaining background emerged from the face of the velocity selector and passed through the collimation system.

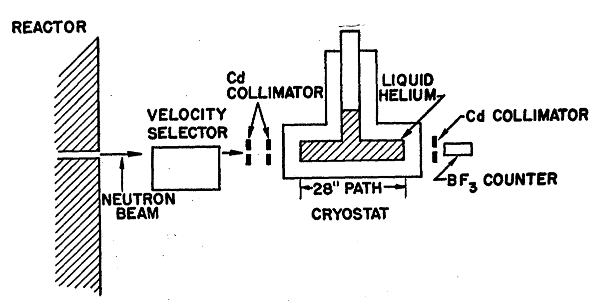

FIG. 1. Experimental arrangement; schematic diagram.

[6] L. Goldstein, Phys. Rev. **83**, 289 and **84**, 466 (1951).
[7] G. Placzek, Phys. Rev. **86**, 377 (1952).
[8] W. H. Keesom and K. W. Taconis, Physica **5**, 270 (1938); J. Reekie, Proc. Cambridge Phil. Soc. **36**, 236 (1940).
[9] J. Reekie and T. S. Hutchison, Phys. Rev. **92**, 827 (1953); Hutchison, Beaumont, and Reekie, Proc. Phys. Soc. (London) **A66**, 409 (1953).
[10] Goldstein, Sommers, King, and Hoffman, in *Proceedings of the International Conference of Low Temperature Physics*, edited by R. Bowers (Oxford, 1951), pp. 88–89.
[11] D. G. Henshaw and D. G. Hurst, Phys. Rev. **91**, 1222 (1953).
[12] H. London and P. A. Egelstaff, Communication at the Third International Conference of Low Temperature Physics and Chemistry, Houston, December 1953 (unpublished).
[13] L. Goldstein and H. S. Sommers, Jr. (to be published).
[14] L. D. P. King, Los Alamos Report LA-1301 (1952) (unpublished).

B. Neutron Velocity Selector

We used a helical velocity selector of the type described previously by two of us.[15] The reader is referred to that paper for a complete description of the instrument and an analysis of the spectral distribution of its transmitted beam.

The present rotor, $11\frac{1}{4}$ inches o.d. by 17 inches long, was composed of alternating disks of $\frac{7}{8}$ inch lucite and $\frac{1}{32}$ inch cadmium. Seventy-two helical slots $\frac{1}{4}$ inch wide and $1\frac{1}{4}$ inches deep were milled into the cylindrical surface of the rotor. These slots had a pitch of 170 inches per radian.

The fractional transmission of the rotor is 60 percent. The single slot transmission function $g(\lambda)$ gives the spectral distribution of the beam transmitted by the selector if the distribution of the incident neutrons is independent of wavelength. $g(\lambda)$ is approximately the triangle shown in Fig. 2. The Maxwellian distribution of the neutrons from the reactor improves the resolution of the beam leaving the velocity selector although the spread of wavelengths still extends from $(\lambda_0/2)$ to $(3\lambda_0/2)$. For this rotor, λ_0 is given in terms of its angular speed ω by the relation

$$\lambda_0\omega = 8.76\times 10^3 \text{ A}-\text{rpm}. \quad (1)$$

The spectral distribution of the beam striking the liquid helium can easily be deduced from $g(\lambda)$ if one knows the velocity distribution of the neutrons leaving the pile. A rough check on this showed that the intensity varied approximately as λ^{-5}, corresponding to the low energy tail of a Maxwellian distribution. For this condition, the neutrons leaving the selector have the wavelength distribution:

$$f(\lambda) = \lambda^{-5} g(\lambda). \quad (2)$$

This line shape, shown in Fig. 2, may be used to derive the resolution ρ, the reciprocal of the resolving power of the instrument, according to

$$\begin{aligned}\rho &= (\langle\Delta\lambda^2\rangle_{Av})^{\frac{1}{2}}/\bar{\lambda} \\ &= (\langle\lambda^2\rangle_{Av} - \bar{\lambda}^2)^{\frac{1}{2}}/\bar{\lambda}.\end{aligned} \quad (3)$$

All averages are evaluated over the distribution $f(\lambda)$, by the general formula

$$\bar{\varphi} = \int_{\lambda_0/2}^{3\lambda_0/2} \varphi(\lambda) f(\lambda) d\lambda \Big/ \int_{\lambda_0/2}^{3\lambda_0/2} f(\lambda) d\lambda. \quad (4)$$

We thus find,

$$\bar{\lambda} = 0.78\lambda_0; \quad \rho = 0.23. \quad (5)$$

It is seen that the Maxwellian character of the pile neutron distribution halves the effective line width.

The transmission of the stationary rotor as measured by our counter was about 2×10^{-6} and gave a background of epi-cadmium neutrons of 13/min at a reactor power of 30 kw. The cadmium ratio of the external beam, measured with our geometry and counter but with the velocity selector removed from the beam, was 150.

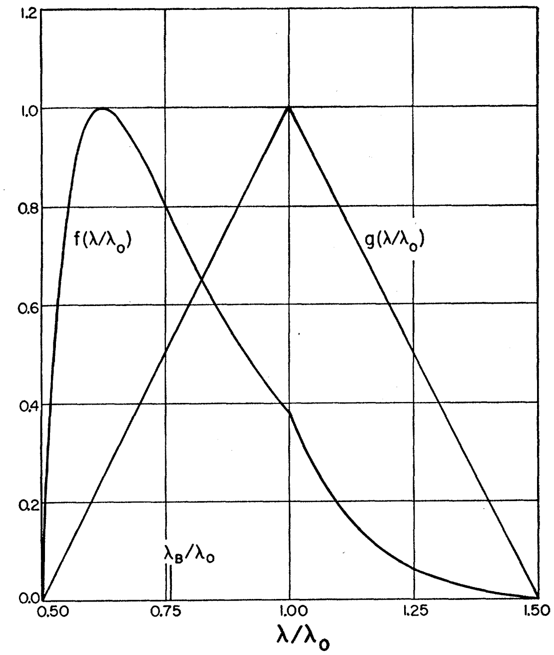

FIG. 2. Characteristics of neutron velocity selector. $g(\lambda/\lambda_0)$, transmission function; $f(\lambda/\lambda_0)$, spectral distribution of transmitted beam.

As described previously,[15] the rotor speed was monitored with a General Radio Strobotac. Unfortunately, the frequency stability of the Strobotac was not sufficient to prevent significant variations of the intensity of the transmitted neutrons. By alternately measuring the intensities of the direct beam and the beam passing through the target, errors due to these small changes in rotor speed were reduced below those associated with counting statistics.

C. Helium Cryostat

Sections through the liquid helium cryostat are shown in Fig. 3. The helium container B is in the form of an inverted T of stainless steel. The horizontal section, through which the neutrons pass, is a cylinder of 2-inch o.d. by $27\frac{7}{32}$-inch length, lined internally with 0.030 inch of cadmium to absorb scattered neutrons. Each end window was turned from stainless steel to a thickness of 0.013 inch. The tube is enclosed with a radiation shield C in thermal contact with the liquid air A. This shield is of copper tubing capped with aluminum end plates 0.090 inch thick. Thermal contact between the vertical stem of the helium container and the liquid air was achieved by the metal plugs E.

In parallel with the horizontal tube containing the liquid helium and fastened to the outside of the radiation shield is the blank tube D, an evacuated replica of the horizontal part of the helium container. By rolling

[15] J. G. Dash and H. S. Sommers, Jr., Rev. Sci. Instr. 24, 91 (1953).

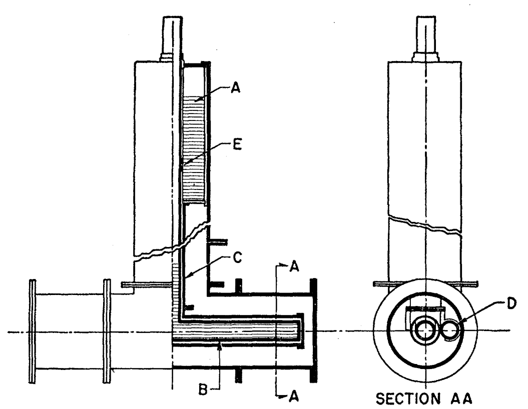

FIG. 3. Helium cryostat; schematic diagram.

the cryostat bench laterally, either the helium or the blank could be interposed in the neutron beam.

3. MEASUREMENTS

A. Wavelength Calibration

Although the velocity selector is an absolute instrument, the difficulties of mechanical alignment, coupled with its low resolution and the uncertainty of the velocity distribution of the incident beam, induced us to calibrate by BF_3 absorption measurements. At suitable rotational speeds, we measured the ratio of the intensities transmitted by our standard BF_3-filled cells to those transmitted by a similar evacuated cell. Figure 4 is a plot of λ_B, the average wavelength measured by boron absorption, against the reciprocal of the rotor speed. The three curves are for the different alignments of the velocity selector that were made during the entire course of the experiment. The relation

$$\lambda_B\omega = 6.7\times 10^3 \text{ A}-\text{rpm}, \tag{6}$$

shown by the broken line, results from averaging the theoretical transmission of the BF_3 standards, in the following way. We define λ_B as the wavelength calculated from the mean boron transmission,

$$\sigma_B(\lambda_B) = -(1/nl)\ln\tau_m(\lambda_B), \quad \lambda_B = \lambda_B(\sigma_B),$$

where n is the numerical density of the BF_3 molecules, l is the absorption length of gas, and $\sigma_B(\lambda_B)$ is the cross section of BF_3 at the monochromatic wavelength λ_B.[16] The mean boron wavelength was therefore computed from the average,

$$\tau_M(\lambda_B) = \int_{\lambda_0/2}^{3\lambda_0/2} e^{-nl\lambda_B(\lambda)} f(\lambda)d\lambda \Big/ \int_{\lambda_0/2}^{3\lambda_0/2} f(\lambda)d\lambda, \tag{7}$$

yielding $\lambda_B = 0.76\lambda_0$. This relation, combined with Eq. (1), yields Eq. (6).

The curvature of the calibration lines is due to an excess depletion of very slow neutrons, perhaps caused by absorption in the active sphere of the reactor or by free fall of the external beam. It is not due to absorption in air, since most of the neutron path is through helium gas.

Because of some uncertainty in the boron cross section, the transmission of each cell was measured over a wide range of velocities with a time-of-flight slow neutron spectrometer.[17] This calibration differed from our computed absorption by an amount yielding a maximum error of 5 percent in λ_B. The difference was ignored and Fig. 4 taken as our calibrations.

B. Dewar Transmission

To a first approximation, the ratio of the intensities transmitted through the two tubes is the transmission of the liquid helium. A second-order correction of (3.1±0.5) percent was applied as a result of the measurements of the relative intensities passed by the cold evacuated tubes. Because the evacuated helium tube could not be held at liquid helium temperature, the second-order correction was obtained from measurements with both tubes at 80°K. The effect of reducing the helium tube temperature from 80°K to 4°K should be negligible, as the following argument indicates. For short wavelengths the principal attenuation by our stainless steel windows is due to coherent scattering; its temperature dependence is given by the Debye-Waller factor and it is unimportant. At long wavelengths, attenuation is mainly given by nuclear absorption,

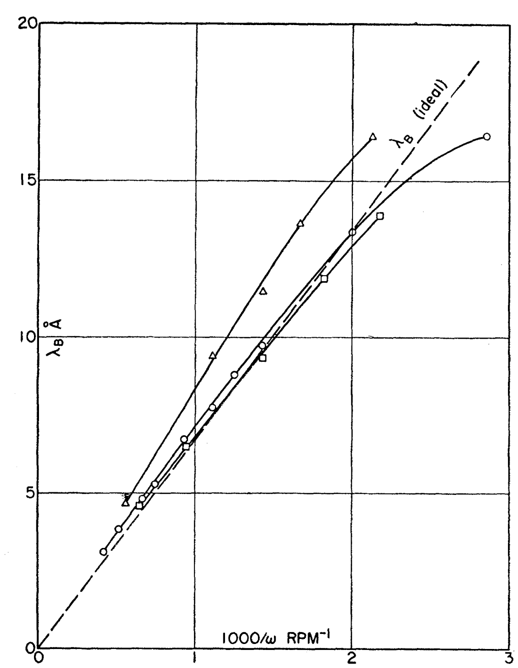

FIG. 4. Neutron velocity selector. Calibration with BF_3 for the three alignments.

[16] Hamermesh, Ringo, and Wexler, Phys. Rev. **90**, 603 (1953); Carter, Palevsky, Myers, and Hughes, Phys. Rev. **92**, 716 (1953).

[17] We wish to thank Dr. H. Palevsky and his group at Brookhaven National Laboratory for calibrating the cells.

TABLE I. Measured transmission of liquid helium.

1.25°K		2.10°K		3.01°K		3.97°K		4.25°K		4.60°K	
λ_B(A)	τ_M	λ_B(A)	τ_M	λ_B(A)	τ_M	λ_B(A)	τ_M	λ_B(A)	τ_M	λ_B(A)	τ_M
4.52	0.474	4.65	0.468	3.12	0.380	3.12	0.415	7.06	0.711	4.63	0.499
5.15	0.551	5.50	0.585	3.80	0.411	3.80	0.435	7.70	0.736	5.20	0.540
5.70	0.628	6.40	0.705	4.33	0.445	4.33	0.463	8.30	0.772	6.00	0.602
6.40	0.719	6.90	0.743	4.90	0.496	4.90	0.498	8.90	0.780	7.00	0.676
7.30	0.802	7.20	0.787	5.46	0.553	5.46	0.551	9.26	0.794	8.00	0.724
8.21	0.873	7.63	0.820	6.06	0.621	6.06	0.602	9.26	0.800	8.40	0.737
8.61	0.900	8.00	0.857	6.75	0.690	6.75	0.674	10.5	0.809	9.00	0.760
9.26	0.922	8.31	0.858	7.62	0.776	7.62	0.740	10.5	0.821	9.70	0.768
9.42	0.926	8.60	0.891	8.81	0.844	8.81	0.793	11.7	0.833	11.0	0.788
9.65	0.925	8.94	0.897	9.92	0.884	9.8	0.819	11.7	0.820	12.0	0.781
9.75	0.938	9.21	0.898	11.3	0.922	10.3	0.837	13.4	0.819	13.4	0.765
10.1	0.953	9.30	0.923	13.1	0.927	11.3	0.853	14.4	0.811	13.4	0.785
10.4	0.953	9.80	0.917	13.7	0.921	11.5	0.854	15.3	0.807	14.9	0.748
11.0	0.966	9.92	0.923	14.8	0.932	13.1	0.853	16.3	0.797	16.3	0.718
11.8	0.970	10.0	0.940			15.5	0.843				
13.9	0.987	10.5	0.958			17.0	0.829				
13.9	0.990	11.3	0.960								
		12.3	0.961								
		13.1	0.965								
		13.6	0.975								
		13.8	0.967								

which is temperature independent. This reasoning is confirmed by our observing the same transmission for the blank tube at 300°K and at 80°K.

C. Transmission of Liquid Helium

The following illustrates a measurement of the transmission of liquid helium. At a particular rotor speed, the neutron flux passing through the liquid was measured over a period of two minutes or for 20 000 counts, whichever took the longer time. Then the cryostat was rolled back to bring the blank tube into the beam; its flux was similarly recorded. These operations, repeated three times, yielded a single transmission; however, if the scatter of either set of readings was outside the computed statistical error, the point was rejected.

The background was taken as the rate at which neutrons reached the counter when the rotor of the velocity selector was stationary. At 30-kw reactor power, the background through the blank tube was 20/min and through the helium 6/min. This reduction of background by scattering in liquid helium indicates that the background was principally due to epithermal neutrons travelling in the beam direction. A small part was also due to slow neutrons emerging from the aluminum face of the velocity selector, for a cadmium sheet in front of the cryostat gave a slight reduction of the background. Since the rate, with the rotor stationary but no cadmium interposed, gives the flux of neutrons with velocities outside of the proper spectrum, we took this rate as the background rate. In even the least favorable case, the signal-to-background ratio was very good; at 17 A it was 720/min to 23/min or a ratio of 31:1.

At short wavelengths, where the neutron flux is high, we reduced the reactor power to keep the counting rates lower than 35 000/min. Checks of counters, including the scale of 100 and the mechanical recorder, indicated that a negligible number of counts was lost at this rate.

Temperatures of the liquid helium were determined by measuring the vapor pressure of the liquid, by Wallace and Tiernan mechanical gauges at vapor pressures above 40 mm of Hg and by a butyl sebacate manometer at vapor pressures below 40 mm of Hg. These vapor pressures were converted into temperatures of the liquid by means of the 1949 temperature scale.[18]

We demonstrated that bubbling of the liquid was unimportant by measuring transmissions of fast (4 A) neutrons just above and just below the lambda point. Also insignificant was multiple scattering of neutrons in the helium.

To check the effect of the lambda transition itself, we made a detailed study in the region of the lambda point, using very slow neutrons (13.8 A). Due to the high transmission of the liquid at this wavelength the accuracy was low, but any change of cross section associated with crossing the lambda point is less than 10 percent.

Transmissions were measured over the wavelength interval 3–16 A for helium temperatures of 1.25, 2.10, 3.01, 3.97, 4.25, and 4.60°K. These are given in Table I. Since each transmission is the ratio of two average counting rates, the probable error in it is the square root of the sum of the squares of the errors in each of the two rates. To this error we added 1 percent for the uncertainty in the transmission of the empty Dewar; the resulting error in the value of the liqiud helium cross section per atom was 0.01 barns, practically independent of the actual value of the cross section.

From the known densities of liquid helium[1] and a helium path length of 69.1 cm, we deduced the total scattering cross sections per liquid atom corresponding to the measured transmissions. These are shown in Fig. 5. The principal features of this graph are a suggested

[18] H. van Dijk and D. Shoenberg, Nature **164**, 151 (1949).

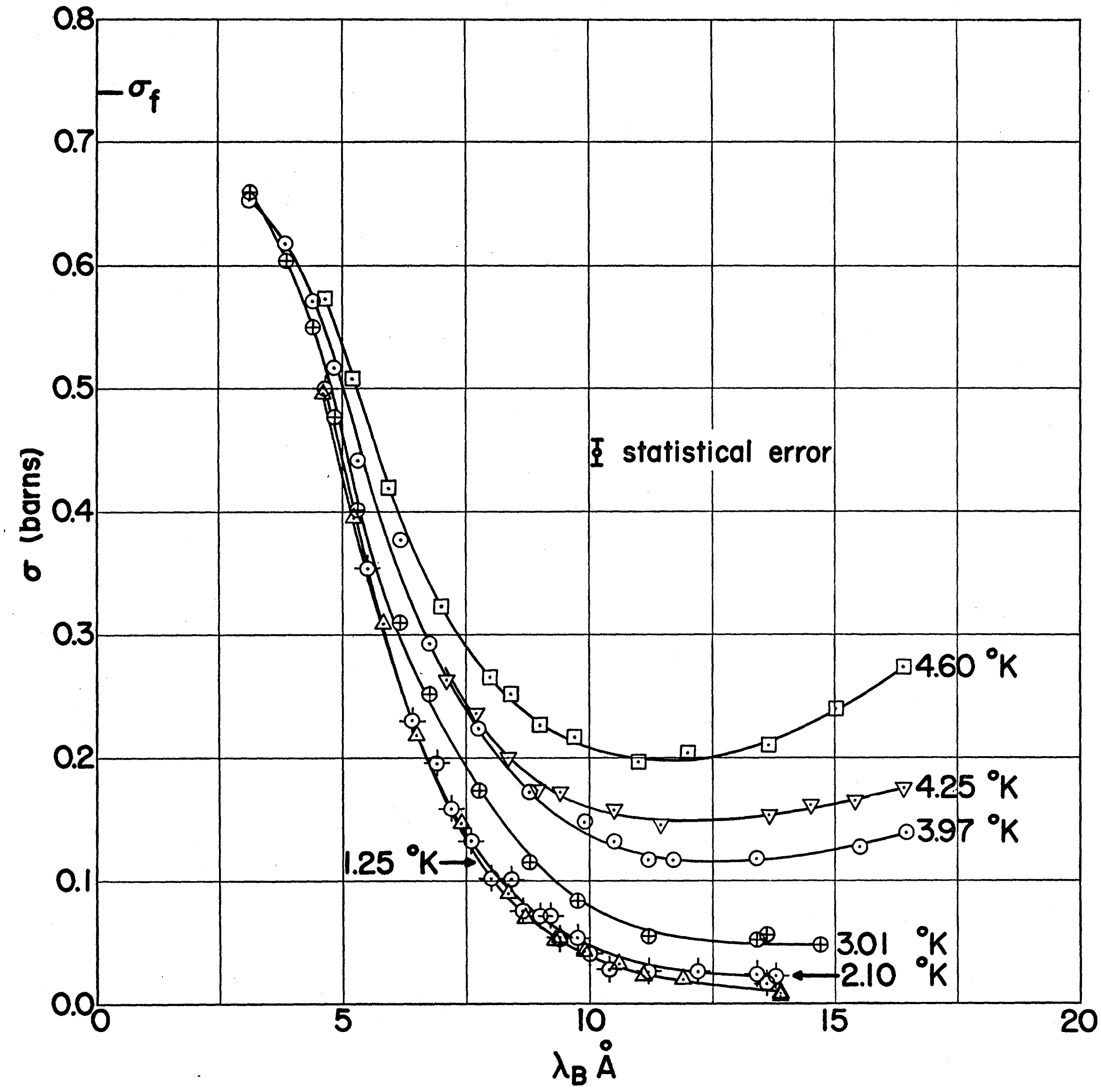

FIG. 5. Measured cross section of liquid helium.

slow drop in cross sections with increasing neutron wavelength from the asymptotic limit, σ_f, of the isolated stationary free atom total scattering cross section, a rapid drop between about 2 and 7 A, a gradual flattening, and finally a rising cross section, at least for the highest liquid temperatures. The decrease in scattering with temperature is clearly demonstrated, with the effect becoming very prominent at long wavelengths.

The values of the long wavelength cross sections at low helium temperatures are somewhat uncertain, not only because of the low statistical accuracy, but also because of the indeterminate amount of absorption by the He^3 in the liquid. Although it is impossible to calculate precisely the concentration of He^3 in the path of the neutron beam, it seems feasible to place an upper limit on this quantity. We accept the value 1.4×10^{-7} as the He^3 concentration in Texas well gas,[19] the gas supply for our liquefiers. This concentration may be assumed constant through the processes of liquefaction and transfer to the experimental Dewar. At temperatures below the λ-point, the "heat flush"[20] creates a flow of He^3 toward the colder portions of the liquid. In the present arrangement, the evaporation at the liquid-gas interface maintained the meniscus as the coldest region of the liquid. The heat flush is consequently directed toward this section, and since liquid was always maintained above the lower end of the standpipe during measurements, the He^3 tended to congregate outside of the neutron beam. This effect, together with the likelihood that the continual pumping reduced the average He^3 concentration, supports the view that the well gas concentration may be taken as an upper limit for these experiments. From the gas concentration, and the

[19] J. G. Daunt, Advances in Phys. 1, 209 (1952).

[20] Soller, Fairbank, and Crowell, Phys. Rev. 91, 1058 (1953).

TABLE II. Smoothed transmission and cross section of liquid helium. τ_M, σ_M, measured transimssion and cross section; τ_c, σ_c, monochromatic transmission and cross section.

λ (A)	1.25°K			2.10°K			3.01°K			3.97°K			4.25°K			4.60°K		
	τ_M	τ_c	σ_c (barns)	τ_M	τ_c	σ_c (barns)	τ_M	τ_c	σ_c (barns)	τ_M	τ_c	σ_c (barns)	τ_M	τ_c	σ_c (barns)	τ_M	τ_c	σ_c (barns)
3							0.379	0.375	0.667	0.410	0.407	0.667				0.448	0.446	0.666
4							0.422	0.405	0.615	0.447	0.437	0.615				0.477	0.469	0.624
5	0.532	0.515	0.440	0.510	0.486	0.476	0.507	0.495	0.478	0.507	0.485	0.537				0.524	0.506	0.562
6	0.668	0.701	0.235	0.650	0.682	0.252	0.616	0.629	0.315	0.602	0.611	0.366				0.601	0.612	0.405
7	0.779	0.831	0.123	0.764	0.812	0.137	0.721	0.762	0.185	0.698	0.746	0.217				0.674	0.709	0.283
8	0.862	0.919	0.056	0.850	0.909	0.063	0.802	0.856	0.106	0.763	0.813	0.154	0.755		0.217	0.726	0.765	0.221
9	0.914	0.963	0.025	0.907	0.956	0.030	0.851	0.900	0.072	0.799	0.840	0.129	0.790		0.182	0.760	0.798	0.186
10	0.944	0.979	0.014	0.940	0.980	0.013	0.890	0.918	0.058	0.829	0.851	0.120	0.811		0.162	0.775	0.804	0.180
11	0.965	0.984	0.011	0.957	0.984	0.011	0.918	0.924	0.054	0.848	0.855	0.116	0.821		0.152	0.785	0.800	0.184
12	0.977	0.985	0.010	0.964	0.978	0.015	0.925	0.925	0.053	0.851	0.851	0.120	0.825		0.148	0.789	0.793	0.191
13	0.985	0.986	0.009	0.965	0.969	0.021	0.928	0.928	0.051	0.848	0.848	0.122	0.823		0.150	0.782	0.782	0.203
14	0.987	0.987	0.009	0.965	0.963	0.025	0.930	0.930	0.049	0.844	0.844	0.126	0.818		0.155	0.764	0.764	0.222
15				0.961	0.961	0.026	0.933	0.933	0.047	0.839	0.839	0.130	0.808		0.164	0.745	0.745	0.243
16				0.961	0.961	0.026				0.835	0.835	0.134	0.797		0.175	0.725	0.725	0.265
17										0.830	0.830	0.138						

published He^3 cross section,[21] we obtain 0.006 barn as the upper limit of the He^3 contribution to the total observed cross section at 14 angstroms. Since this upper limit is well within the estimated probable error of 0.01 barns, we shall neglect the influence of He^3 absorption.

The measured transmission τ_m is an average value over a considerable wavelength spread. To give a better value of the transmission for monochromatic neutrons, we made a correction for the finite resolution of the velocity selector. The desired monochromatic transmission is $\tau_c(\lambda)$. The transmission $\tau_m(\lambda_B)$ measured at the boron-determined wavelength λ_B is the average of the monochromatic transmission, as indicated in Eq. (7). A first-order correction for the finite line shape may be made on the following basis. We write

$$\tau_c = \bar{\tau} - \delta\tau, \quad \delta\tau \equiv \bar{\tau} - \tau_c,$$

defining the first order correction $\delta\tau$. Approximating $\delta\tau \simeq \langle \delta\tau \rangle_{Av} = \langle \bar{\tau} - \tau_c \rangle_{Av}$, we obtain

$$\tau_c \simeq \bar{\tau} - \int_{\lambda_0/2}^{3\lambda_0/2} (\bar{\tau} - \tau_c) f(\lambda) d\lambda \Big/ \int_{\lambda_0/2}^{3\lambda_0/2} f(\lambda) d\lambda,$$

or

$$\tau_c(\lambda_B) \simeq 2\tau_M(\lambda_B) - \int_{\lambda_0/2}^{3\lambda_0/2} \tau_M(\lambda_B) f(\lambda_B) d\lambda_B \Big/ \int_{\lambda_0/2}^{3\lambda_0/2} f(\lambda_B) d\lambda_B. \quad (8)$$

Equation (8) was solved for the approximate corrected transmissions in the range 3–10 angstroms, where the transmissions varied rapidly with the wavelength. These calculated values of τ_c were then used to compute the average transmissions, which were compared with the measured values. The largest disagreement between these calculated average transmissions and the corresponding measured τ_m was 1.6 percent. The transmissions τ_c between 3 and 10 angstroms were therefore accepted as the monochromatic functions, and joined smoothly to our measurements at longer wavelengths.

Table II gives these monochromatic transmissions $\tau_c(\lambda)$ for even integral wavelengths, together with interpolated values of the measured transmissions τ_m and corrected cross sections σ_c. While the corrected cross section curves exhibit a slightly steeper drop and more pronounced minimum, Fig. 5 is still a good qualitative representation of the monochromatic cross section.

We remeasured σ_f, using neutrons transmitted by cadmium, and found

$$\sigma_f = 0.74 \pm 0.04 \text{ barns}.$$

This agrees with the faster neutron value[22] of 0.8±0.2 barns and the bound atom cross section[23] of 1.1±0.15 barns, corresponding to 0.70±0.10 barns for σ_f. It is also in agreement with our previous measurement obtained with the unmodified thermal beam.[10]

4. QUALITATIVE DISCUSSION OF RESULTS

A. Comparison with Neutron Scattering by Solids[24]

The general shape of the total scattering cross section as a function of the neutron wavelength, Fig. 5, is strikingly similar to the scattering cross section curves observed with solids. This suggests that the rapid drop of cross section with increasing neutron wavelength is due to the rapid change of interference scattering on crossing the "Bragg edge." In liquids the "Bragg edge" is not due to a sharply defined lattice spacing of the solid type but to a distance resulting from the averaging over spacings between first, second, etc., ··· neighbors.

[21] L. D. P. King and L. Goldstein, Phys. Rev. **75**, 1366 (1949).

[22] Bashkin, Petree, Mooring, and Peterson, Phys. Rev. **77**, 748 (1950).

[23] A. W. McReynolds, Phys. Rev. **84**, 969 (1951).

[24] For a discussion of the solid model scattering by liquid helium see L. Goldstein and D. Sweeney, Phys. Rev. **80**, 141 (1950).

It is the destructive interference of the scattering from the different atoms which causes the fall in cross section at the "Bragg edge." The higher the liquid temperature, the larger the density fluctuations; since these reduce the destructive interference effects, the scattering should increase with liquid temperature. The large drop in cross section should disappear in the critical region as the critical neutron opalescence effect sets in.[6]

In the limit of very slow neutrons, to within presumably small terms depending on the binding of the liquid atoms, one obtains[13]

$$\lim_{v\ll \bar{v}_A(T)} \sigma(v,T) \sim \sigma_f\left(1+\frac{m}{M}\right)^2 \{(\bar{v}_A(T)/v)+[n(T)kT\chi_T-1]\}, \quad (9)$$

where v is the neutron velocity, $\bar{v}_A(T)$ is the mean atomic velocity in the liquid at temperature T, m and M are the neutron and atomic masses, n is the mean atomic concentration in the liquid, k is Boltzmann's constant, and χ_T is the isothermal compressibility. The first term on the right-hand side is a relative motion or Doppler effect term, and the last one is the very long wavelength limit of the interference term.[6] Even though our wavelengths are probably not long enough for this limit to have been reached, the increasing cross section with wavelength for the 4.6°K helium may be due to the increasing size of the first Doppler term. This limiting $1/v$ dependence of the cross section is of great generality, for it is valid in all thermodynamic phases.

B. Comparison with Scattering by Gases

The qualitative behavior of our cross sections bears no resemblance to the scattering by an ideal Boltzmann gas, which is wavelength independent except for the Doppler correction. Nor is there a resemblance to the scattering by an ideal Bose-Einstein fluid,[25] in which the cross section rises above σ_f. The latter conclusion was deduced in the preliminary work.[10] While the ideal Bose-Einstein fluid model is useless here, this does not mean that the statistics are unimportant for the theoretical description of other properties of liquid helium. It merely indicates that as far as scattering processes are concerned, the binding of the atoms plays a dominant role.

[25] Goldstein, Sweeney, and Goldstein, Phys. Rev. **77**, 319 (1950).

C. Remarks on Some Results Based on the Landau Hydrodynamic Model of Liquid Helium

We wish finally to mention the predictions of Akhieser and Pomeranchuk[26] based on the Landau hydrodynamic model of liquid helium, even though our results do not permit a comparison with them. These authors calculate scattering cross sections associated with the production of a phonon and scattering by rotons for neutrons of velocity considerably smaller than the sound velocity s in liquid helium ($\sim$240 m/s) or with wavelengths much larger than 17 A. The calculated phonon production cross section, though depending inversely on the neutron velocity v, is extremely small, of the order of $(10^{-6}s/v)\sigma_f$ at 1.0°K, and may be disregarded. The scattering by rotons is dealt with as an elastic collision leading to a cross section independent of neutron energy and depending linearly on the number of rotons present in the liquid. At 1 and 2°K the roton cross sections are given as $7\times10^{-5}\sigma_f$ and $3\times10^{-3}\sigma_f$, respectively. The energy independence of the roton cross sections at these very long neutron wavelengths results from considering the normal fraction of the liquid to be a collection of stationary free rotons. The theoretical roton cross section at 2°K is about 10 percent of the one we observe at 14 A; it drops extremely rapidly with temperature.

At very long neutron wavelengths where the above calculations should be valid, the Doppler effect on the scattering by the Maxwellian roton gas cannot be neglected. One expects an increase of the roton scattering cross section with decreasing neutron velocity, tending toward the "$1/v$" behavior. In this wavelength range, entirely beyond the one used in this work, one can verify the presence of roton scattering below the lambda point.

ACKNOWLEDGMENTS

We are indebted to Dr. L. D. P. King for actively participating in the early planning of the experiment. We wish also to thank the reactor group, the liquefier group, and the machinists for their cooperation. We acknowledge the assistance of Dr. C. J. Hoffman who helped in the assembly and testing of the cryostat, and of Mr. T. E. Carman for the mechanical design of the velocity selector. Mr. Max Goldstein and the computing group with Miss M. L. Johnson, Mrs. J. E. Powers, and Mrs. A. M. Snowden collaborated in the numerical work and preparation of graphs.

[26] A. Akhieser and I. Pomeranchuk, J. Phys. (U.S.S.R.) **9**, 461 (1945).